JST&M 10(2026), 1– 14
DOI: 10.57131/jstm.2026.10.1

Original scientific paper

ASSESSING ANTIBACTERIAL EFFICACY OF NANOPARTICLES FROM THREE PLANT EXTRACTS AGAINST *E.COLI* AND *STREPTOCOCCI* IN URBAN WASTEWATER

Elton Yerima Ngu[1,2], Julson Ahmed Tchio[3], Kamseu Eli[2], Tsamo Cornelius[1]

[1]Department of Agricultural and Environmental Engineering, College of Technology, University of Bamenda, [2]Laboratory of Materials, Local Materials Promotion Authority, [3]University of Oulu, Fibre and Particle Engineering Research Unit, Finland

ABSTRACT

Silver nanoparticles (Ag-NPs) obtained through green syntheses are gaining remarkable interest in water treatment due to their excellent chemical, physical, and biological properties. Ag-NPs were synthesized using three plant extracts: *Carica papaya*, *Vernonia amygdalina*, and *Perilla frustescens var* as reducing agent, and 6 mM of silver nitrate as precursor. The extracts demonstrated a good potential to reduce Ag(+1) to Ag(0) for Ag-NPs synthesis. Characterization of synthesized Ag-NPs was achieved through UV-Vis spectroscopy, Fourier Transform Infrared analysis, X-ray diffraction, optical microscopy, and zeta potential. The Surface Plasmon Resonance (SPR) was between 410 and 440 nm. The optical microscopy confirmed the presence of nanoparticles (NP) and an aggregate of NP. The synthesized NPs had a crystalline structure, confirmed by the XRD spectra. The average surface charge of NPs was negative (< -10 mV), indicating a potential for aggregation of the three NPs, as confirmed by the particle size distribution. Their antibacterial activities against *E. coli* and *Streptococci* were analyzed in urban wastewater. They exhibited good antibacterial properties, with BNPs being most effective at inhibiting both bacteria, followed by PNP and VNP. This reveals that NPs produced from different plants have different yields, properties, and antibacterial activities, and, most especially, can be used in water and wastewater treatment..

Keywords: *Carica papaya, Vernonia amygdalina*, *Perilla frustescens var*, Ag-NPs, green synthesis, characterization, antibacterial agent

Corresponding Author:
Elton Yerima Ngu,
College of Technology, University of Bamenda
Yaounde - Cameroon
Tel.: 237670803969
E-mail address: nguyerims@gmail.com

1. INTRODUCTION

Nanotechnology has demonstrated diverse applications across a wide range of scientific and technological fields and has emerged as a rapidly growing area of research and innovation. Nanotechnology typically deals with materials possessing at least one dimension below 100 nm [1]. Conventional methods for synthesizing nanoparticles include physical techniques (such as vapor deposition and lithographic processes) and chemical approaches (such as borohydride

and citrate reduction methods). However, these methods often result in relatively large particles with poor monodispersity, and the processes have been reported to pose environmental hazards [2,3]. However, the biological method of synthesis, which is the most recent method, has attracted a lot of attention because it is safe (nontoxic process), cost-effective, and requires less time than other methods [4]. The biological process of synthesizing nanoparticles is mainly through the process of precipitating the nanoparticles of metals like Silver (Ag), Gold (Au), Platinum (Pt), etc., with organic matter like plants, bacteria, and fungi [3, 5].

The area of most interest in the biosynthesis of metal nanoparticles within the last decade is the application of plant extract in the synthesis reaction. Antioxidant biochemicals such as terpenoids, alkaloids, phenolics, aldehydes, proteins, and amino acids are present in plant extracts, which are capable of reducing metal ions to nanoparticles and stabilizing them [6, 7]. Moreover, plants are readily available, hence extracts can be easily obtained, enabling scaling up production. Several documents are available on the development of metal nanoparticles using plant extracts [7, 8-10]. However, silver nanoparticles have emerged to be the most effective because it has a good and broad spectrum of antimicrobial activities against viruses, bacteria, and other microorganisms, and they also have minimal toxicity to human cells [7]. Available reports covering the scope of the modalities to biosynthesize Ag-Nanoparticles of different shapes and characteristics from plant extract have been established [11-14], and their excellent antimicrobial characteristics against: *Staphylococcus aureus, Escherichia coli* [15, 16], *P. aeruginosa*, *K. pneumonia* [16] amongst others, have been observed in cultured mediums. Present interest is in Ag-NP synthesis from three plants, namely: Bitter leaf plant (*Vernonia amygdakina*), Pawpaw plant (*Carica papaya*), and Perilla mint (*Perilla frutescens var*). Extracts from different parts (fruit, leaves, flowers, callus, seed, peel and bark) of these plants have been used for the synthesis of Ag-NP in different studies and they have shown to have incredible antimicrobial and antibacterial properties to bacterial such as: gram-positive and gram-negative bacterial [17-19], *E-coli* and *Staphyloccocus* [20-22]; coliform [23], oral bacterial [24], anticancer [22, 25] and also in colorimetric experiments to determine heavy metals in solution [26]. Even though there is some study on the application of Ag-NP produced from these three plants in inhibiting microbial or bacterial action or eliminating them, it has mostly been applied in the medical domain and in controlled environments, such as diffusion methods. Also, there are few or no studies available on the application of Ag-NP produced from these plants in industrial, urban, or domestic wastewater treatment.

The present study aims to achieve the following objectives:

1. Synthesize silver nanoparticles from three different plants: *Carica papaya* (Paw-paw plant), *Vernonia amygdalina* (Bitter leaf plant), and *Perilla frustescens var* (Perilla mint plant).
2. Characterize the silver nanoparticles by UV-VIS spectroscopy, Fourier-transformed infrared spectroscopy (FTIR), X-ray diffraction, and zeta potential.
3. To compare the antibacterial properties of the silver nanoparticles against *E.coli* and *Streptococcus* in domestic wastewater.

The key findings of this work are related to the comparative study of the antibacterial activities of Ag-reduced nanoparticles using three plant extracts.

2. MATERIALS AND METHODS

2.1. Collection of plant materials

The samples of interest for synthesizing silver nanoparticles were from three different plant types. The paw-paw plant (*Carica papaya*), bitter leaf plant (*Vernonia amygdalina*), and Perilla mint plant (*Perilla frutescens var*). These plants were selected

because they are traditionally regarded as medicinal plants in rural Cameroon and are used in the treatment of diseases such as typhoid fever, hemorrhoids, ringworm, and various other ailments. Plant samples were obtained from a farmland around the military base in Yaounde, commonly known as "Quartier Gènèral". To ensure consistency of content and reproducibility of results, a one-time sampling was done around the sample area, where for each plant, several samples were jointly collected. The plants were washed with deionized water 3-4 times and exposed to sunlight for about 14 days to lose humidity and dry up. Samples were rewashed to remove dust particles that may have accumulated during drying. The samples were then placed in an oven at 50 °C to dry slowly. After drying, samples were crushed and preserved in labeled plastic bags.

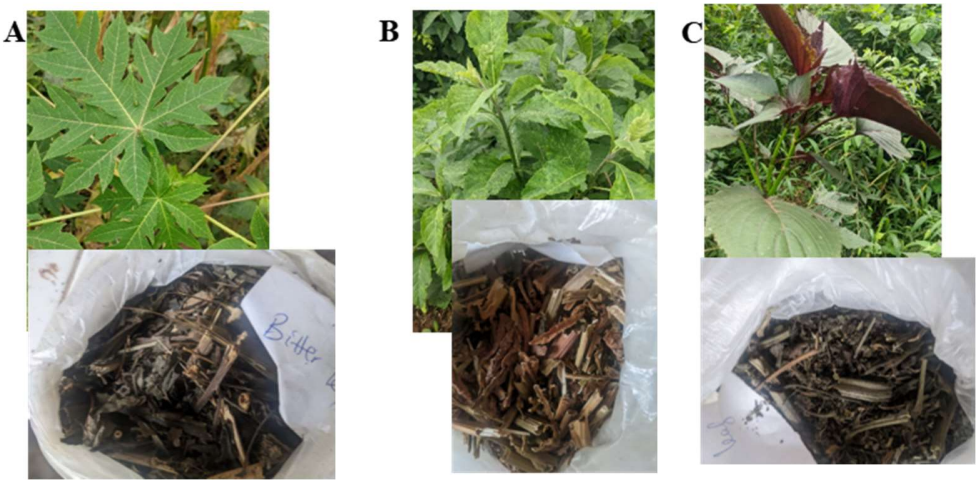

Figure 1. Plant Samples used in the synthesis of Ag-NPs: (A) *Carica papaya*: (Pawpaw plant); (B) *Vernonia amygdalina*: (Bitter leaf plant); (C) *Perilla frutescens var*: (Perilla mint plant)

2.2. Collection of extracts from plants and preparation of a solution

Plant extracts were obtained using an adopted and modified procedure from Maged et al. [15]. 20 g of each crushed plant sample was placed in a 1000 ml Erlenmeyer flask, and 400 mL of deionized water was added to it. The flask and its content were then placed on a heater at 60 °C and stirred at 500 rmp for 60 minutes (1 hour). When the color of the solution turned brown, it was allowed to cool at room temperature, then filtered with a Whatman filter paper to remove all plant particles. The extracts were then preserved at 4 °C to be used later for bio-nanoparticle synthesis.

According to Maged et al. [15], the concentration of silver nitrate with optimal reduction characteristics and the best antibacterial properties is 6 mM. Analytical grade Silver Nitrate reagent (99.5% purity level), was commercially purchased. The silver salt used did not need any further purification. Distilled water was used to make the solution. A solution of silver nitrate with the prescribed concentration was prepared by dissolving the appropriate amount of the silver salt into distilled water, stirring until the solution was homogeneous, and sealing the solution to prevent any contamination.

2.3. Biosynthesis and characterization of Silver nanoparticle (Ag-NP)

The Ag NP were synthesized by putting 2 mL of leaf extract in their respective labeled sample container. 50 mL of 6 mM silver nitrate solution was added to the leaf extract and allowed to sit at room temperature. The

reaction was followed up for over a period of 4 hours.

The composition, size, and morphology of the synthesized Ag-NPs were determined through various characterization methods. To determine the formation of Ag-NPs, UV-VIS spectrometry was done on each sample after 24 hours. A quartz cuvette with a 1 cm optical path was used with a wavelength range of 300 – 600 nm. The morphology and size of the Ag-NPs were observed by means of optical microscopy. For evidence of Ag in the nanoparticles, X-ray diffraction analysis was done on the Ag-NPs.

2.4. Characterization of antibacterial properties of nanoparticles

For characterization of the nanoparticle's antibacterial properties, the nanoparticles were used to treat domestic wastewater. Wastewater was sampled from a municipal waste stream in Bonamoussadi, Yaounde, Cameroon. Six plastic bottles were cleaned with distilled water, and into each container, 1 L of the wastewater sample was introduced. 30 mL of nanoparticle solution from the three plant extracts was poured into three containers, each in its own container, and labeled: VL1 (wastewater + Perilla mint NP), PP1 (Wastewater + Pawpaw plant NP), and BL1 (wastewater + Bitter leaf NP). An equivalent amount (30 mL) of silver nitrate in one container (Ag(1+): Wastewater + AgNO3) and finally plant extract in another (EXT: wastewater + Plant extract). A container of wastewater (WW) was used as a reference. Each container and its contents were allowed to stand for 24 hours at room temperature. The cup-plate agar diffusion method was used to E-coli and Streptococci load in water samples [15].

3. RESULTS AND DISCUSSION

The study on the green synthesis of Ag nanoparticles using bitter leaf plant, pawpaw plant, and Perilla plant extracts was done and systematically reported in this report. The aqueous Ag+ was reduced to silver nanoparticles upon the addition of natural plant extracts. The colors observed during the transition of the reaction were from pale yellow to a brown solution with precipitate settling at the bottom of the solution within 5 hours of reaction. No further changes were detected for another 12 h; however, the majority of the precipitates had settled, and the solution became clearer.

3.1. UV-VIS characterization

The confirmation of the formation of silver nanoparticles was monitored using UV-VIS spectrometric analysis (UV752(D) PEC Medical USA UV/VIS photospectrometer). The UV-VIS spectra (Figure 2) of silver nanoparticles from the three plant extracts showed an increase in absorbance with an increase in wavelength from 300-600 nm, with an intense Surface Plasmon Resonance (SPR) observed at 410 and 440 nm, and are in the range for the stipulated absorption wavelength of Silver. This conforms to the findings of Logeswari et al [16], who indicated that the maximum absorption of silver nanoparticles within this wavelength range confirms their formation. Furthermore, the band of the silver nanoparticles spectra was similar, which would indicate a similarity in average particle size and shape as stipulated by Bamsaoud et al. [27] and Mage et al. [15]. However, the absorption peak of Pawpaw extract Ag-nanoparticles (PNP) was identified to have a red shift and decrease in intensity, which could be attributed to the increase in particle size of this nanoparticle, compared to the other two. Furthermore, the alignment of the peaks of BNP and VNP would indicate their particle size falls within the same range; however, given that the absorption peak of BNP is more intense, this might insinuate the high concentration of BNPs, which are more stable with the smallest size compared to the other two [28]. Hence, the UV-VIS absorption peak reveals that nanoparticles produced from bitter leaf plant extract (BNP) are more stable, with a quick formation of nanoparticles, a higher concentration of nanoparticles, and the

smallest size. This is closely followed by nanoparticles produced from Perilla extract (VNP), and finally, those from pawpaw plant extract (PNP). This would indicate that different plants subjected to the same conditions for the green synthesis of nanoparticles have different formation kinetics, size, and shape. This difference in formation kinetics might be attributed to the unique phytochemicals of each plant based on the concentration of reducing agents (polyphenol, flavonoids, and tannins) in each plant [29].

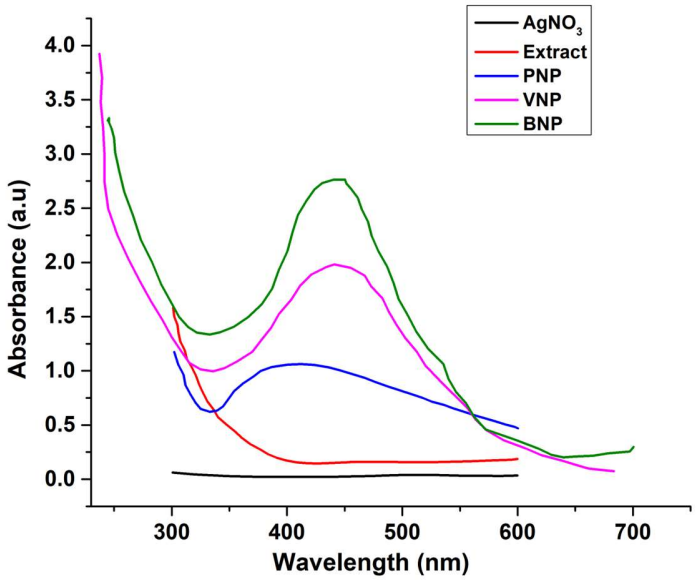

Figure 2. UV-VIS Spectra of Silver nitrate ($AgNO_3$), Plant extract (Extract), and Ag-NPs (PNP, VNP, BNP), *PNP: Pawpaw plant Ag-nanoparticles; VNP: Perilla plant Ag-NP; BNP: Bitter leaf plant Ag-NP*

The UV-VIS spectroscopic analysis also has the possibility of determining the size and shape of nanoparticles. The absorption spectra of the synthesized nanoparticles revealed peaks in the range of 410 – 440 nm. According to Martínez-Castañón et al. [30], nanoparticles with absorptions within this range are mostly characterized by a spherical shape and a size range between 7 and 30 nm. Which fall within the size range of nanoparticle materials.

3.2. Fourier Transform Infrared (FTIR) Spectroscopy analysis

The FTIR analysis investigates and identifies the functional groups present in both plant extract and Ag-NPs, as well as reveals factors responsible for capping and possible interactions between silver and bioactive molecules. The FTIR spectrometry data were obtained at the inorganic laboratory of the University of Yaounde 1 (Cameroon) using the BURKER OPTIK ALPHA Spectrometer (standard glass cells and Borosilicate glass windows). This analysis depends on the principle that electromagnetic energy in the infrared region, ranging from 4000 – 400 cm^{-1}, is absorbed by particles, causing the subatomic particles to vibrate. Figure 5 presents the FTIR spectrograph of the synthesized Ag-NPs from all three plants. Based on the FTIR peaks characterization, the peak position reveals the form of nanoparticles, while the intensity of the peak determines the size of the nanoparticles [31, 32]. The FTIR spectrum reveals a broad and intense band from 3800-3000 cm^{-1} with a peak at around 3302 cm^{-1}, which may probably be due to the stretching or bending vibration of the hydroxyl groups (O-H) of polyols such as Glycerol, Mannitol, hydroxyflavones, and catechins, or the vibration of O-H of water

molecules on the surface of the Ag-NPs [33]. Absorption band at 1636 cm^{-1} may correspond to the C=O stretching vibration of the carbonyl group (-C=O), which may indicate either the presence of carboxylic acids or amides [34, 35]. These phytochemicals have been reported to be present in plant extracts and are primarily responsible for the bioreduction of Ag ions to Ag-NPs, contributing to their stabilization and the provision of a capping agent that prevents agglomeration of Ag-NPs [36, 37]. Finally, the peak at 415 cm^{-1} could be attributed to the stretching vibration of Ag-O of silver oxide or might suggest interactions between silver nanoparticles (Ag-NPs) and oxygen-containing functional groups in accordance with the findings of Kayed et al. [38]. This might also imply the stabilization of Ag-NPs by organic compounds containing oxygen.

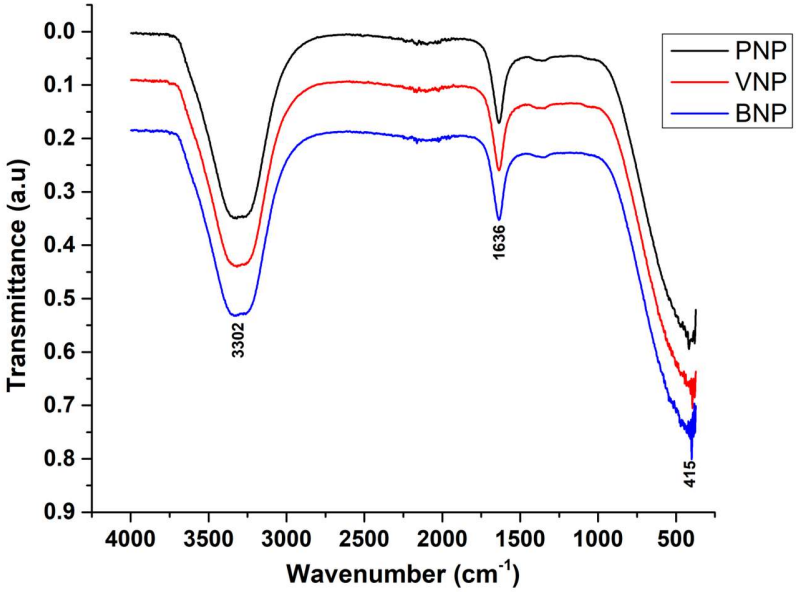

Figure 3: FTIR analysis of synthesized Ag-NPs

3.3. X-ray Diffraction analysis

This analysis is an essential technique to determine the crystalline nature of the nanoparticles. X-ray analysis was done in the Department of Engineering Enzo Ferrari University of Modena. It was performed using a Bruker D8 Discover, Japan, Cu-Kα radiation at 40 kV and 30 mA, θ to 2θ configuration. Spectral measurements were performed in the angular range of 5°–80° (2θ/min). Figure 4 shows the X-ray diffractogram of the Ag-NP produced from the three plant extracts, to confirm their crystal characteristics. The diffractogram of the Ag-NPs confirmed its crystalline characteristics. Major peaks were observed around the following angles; 23.02°, 26.4°, 34.4°, 37.86°, 40.68°, 49.12°, 54.2°, 56.56°, and 76.06°. Referencing from the International Center for Diffraction Data (ICDD), these peaks corresponds to the silver crystalline phases in the plane (111), (220), (200), (220), (311), (222), (440) respectively, and are attributed to the face-centered cubic (FCC) crystal structure. These results corroborated the data obtained from the standard ICDD database having card no: #00-004-0783. Of all the phases, the most important is the (111) plane configuration, which indicates the Ag-NPs are well crystalline and stable. The unassigned peaks phases marked "X" and others in the figure may be due to the crystallization of bioorganic phases present in these plants, according to Asif et al. [39].

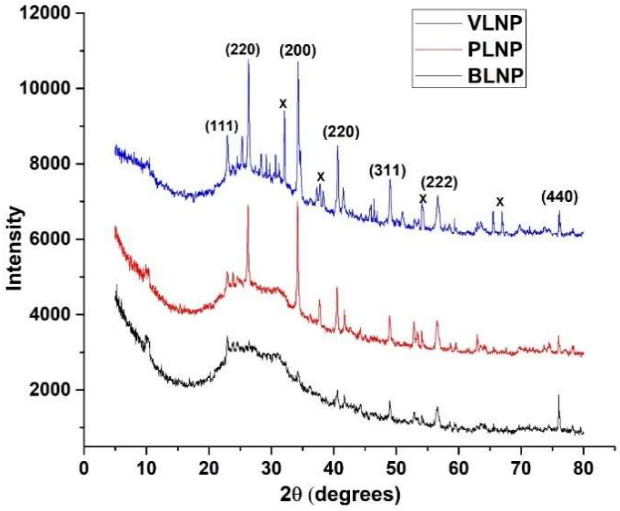

Figure 4. X-ray diffractogram of synthesized Ag-NPs

3.4. Microscopy of Silver nanoparticles

Microscopy is a surface imaging method that is essential in determining the particle size distribution, particle structure, and surface morphology of the synthesized nanoparticle. In this study, optical microscopy was used to determine the morphology of the Ag-NP from the three plant extracts (Figure 5). The optical microscopy was done in Oulu University, Finland, using Dark-field microscopy (DFM). It operates through selectively capturing light scattered from the sample while excluding the incident light. As a result, the field around the sample produces a dark background while the sample is visualized as a bright object [40, 41]. Observations were done at 250 µm, 100 µm, and 50 µm. It could be observed that the Ag-NPs from the 3 plant extracts were formed, which are dense, not too dispersed, and agglomerated in certain regions, with different sizes of nanoparticles. Agglomerations could be a result of the solvent effect of Van der Waals attraction between particles in solution, causing them to form little clusters. Optimal microscopic analysis was only able to observe the presence of nanoparticles in solution. However, scanning electron microscopy (SEM) and transmission electron microscopy (TEM) are required to observe a more detailed surface morphology of the nanoparticles for their shape and size.

3.5. Particle size distribution and Zeta potential analysis

This is an essential analysis that determines the electrical potential of nanoparticles in colloidal dispersions to define their charge in suspension. Zeta potential was measured by adding Ag-NP solution to a cell that contains two gold electrodes. When a voltage was applied to the electrode, the particles moved towards the electrode with the opposite charge. A Doppler technique was used to measure the particle velocity as a function of voltage. A laser passes through the cell, and as particles move through the laser beam, the intensity of scattered light fluctuates at a frequency proportional to the particle speed. Particle speed at multiple voltages was measured, and the data were used to calculate the zeta potential. This reveals the surface charge, stability, and aggregation of nanoparticles. The average zeta potential of the synthesized nanoparticles was -7.142 mV, -6.082 mV, and -1.424 mV for BLNP, PLNP, and VLNP, respectively (Figure 6).

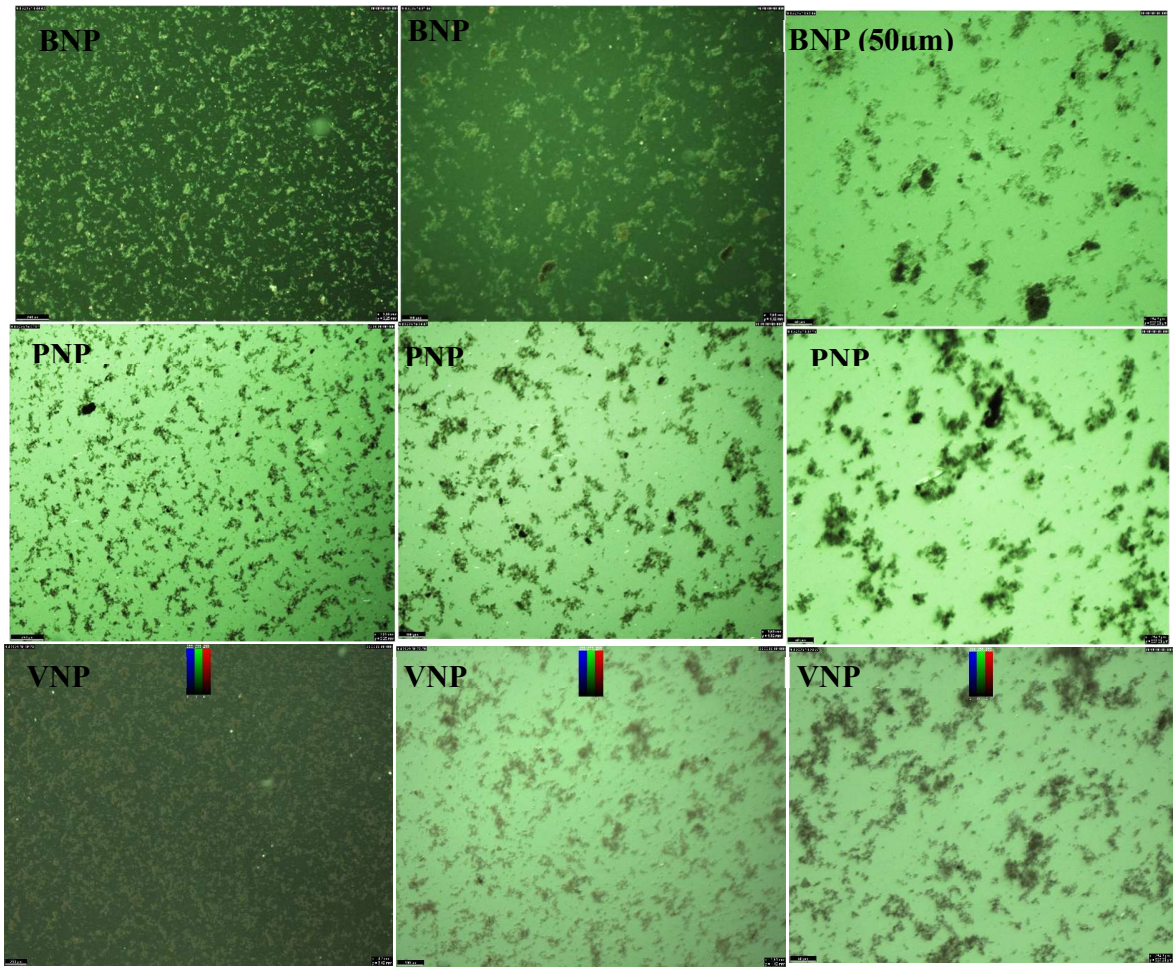

Figure 5. Optical microscopic imaging of synthesized nanoparticles: *BNP (Bitter leaf plant extract NP), PNP (Pawpaw plant extract NP),* and *VNP (Perilla mint extract NP)*

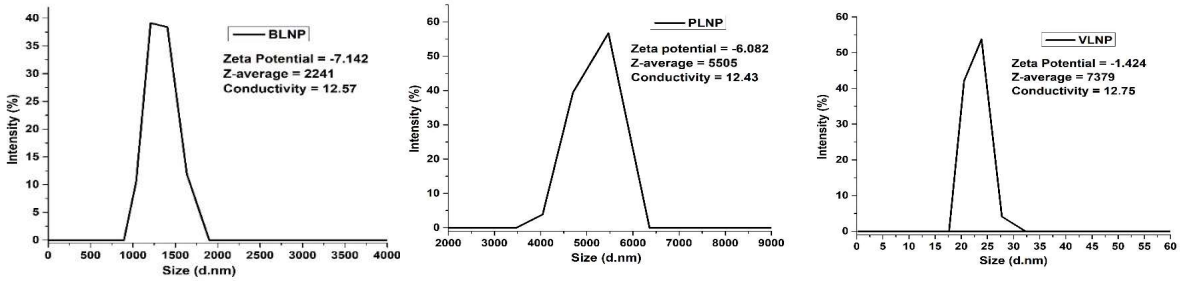

Figure 6. Particle size distribution – Zeta potential of synthesized nanoparticles

The negative zeta potential of the Ag-NPs would indicate that the net charge on the surface of the nanoparticles is negative. Furthermore, the values were observed to be less than 10 mV, indicating the nanoparticles are unstable with weak repulsion forces between suspended particles, limiting dispersion [42]. This may be an indication of the high particle size values of the synthesized particles, given that there was an

aggregation of particles, which confirms the microscopy observations. However, Ag-NP produced from bitter leaf (BLNP) had the highest potential, indicating it has the most stability, while VLNP had the least potential, indicating the least stability of the three synthesized Ag-NPs.

3.6. Evaluation of antibacterial properties of nanoparticles

The antibacterial efficiency of silver nanoparticles has been mostly observed either in medical applications, microbial incubated treatment [15, 27], or cultured bacterial treatment [3], where nanoparticles are being used to treat one, at most three microbes at a time. However, there is very limited literature or works on the determination of antibacterial properties of silver nanoparticles in standard wastewater. The silver nanoparticles (Ag-NP) synthesized in this study were tested for their efficiency to eliminate *E. coli* and *Fecal Streptococci* from domestic wastewater. Figure 7 presents the effect of synthesized silver nanoparticles, plant extract used for nanoparticles synthesis, and silver nitrate in wastewater on bacteria in domestic wastewater. Three groups of tests were carried out: nanoparticles in wastewater (VL1, PP1, and BL1), plant extract in wastewater (EXT), and silver nitrate in wastewater (Ag(+1)). The antibacterial properties were evaluated for two bacteria, *E. coli* and *Fecal Streptococci*. When the silver nanoparticles and silver nitrate were introduced into wastewater, the color of the mixture changed from grey to a deep red solution (VL1, PP1, and BL1), but brown for the wastewater in which silver nitrate was added (Ag(1+)) (Figure 7). The change in this color might be due to the influence of their optical properties, due to interactions of the organic and inorganic composition in wastewater, and the Ag (0) and Ag (+), affecting the aggregation and dissolution of NPs, which is in accordance with the findings of Gibson (2018). Alternatively, this might be due to the formation of larger nanoparticles as a result of the reduction of the remaining Ag (+) in solution to Ag (0) by organic contents in water, resulting in a darker solution [43, 44].

Figure 7. Appearance of wastewater upon addition of green-synthesized nanoparticles; *WW: Raw wastewater, EXT: Wastewater + Extract, AG(1+): Wastewater + $AgNO_3$, VL1, PP1, BL1: Wastewater + Silver nanoparticles*

Figure 8 presents the antibacterial analysis of the treated wastewater samples and the wastewater. Figure 8A presents the inhibition zones of Ag-NP on E. coli. It could be observed that the highest inhibition was found in BL1 (BL1 (*E-coli*)), followed by PP1 (PP1 (*E-coli*) and VL1. WW and EXT had high concentrations of *E. coli* (little or no inhibition). Figure 8B presents the inhibition zones of Streptococci in the samples. It could be observed that the highest inhibition of Streptococci was in BL1, followed by VL1, PP1, and Ag (1+). The highest concentrations of *Streptococci* were found in WW.

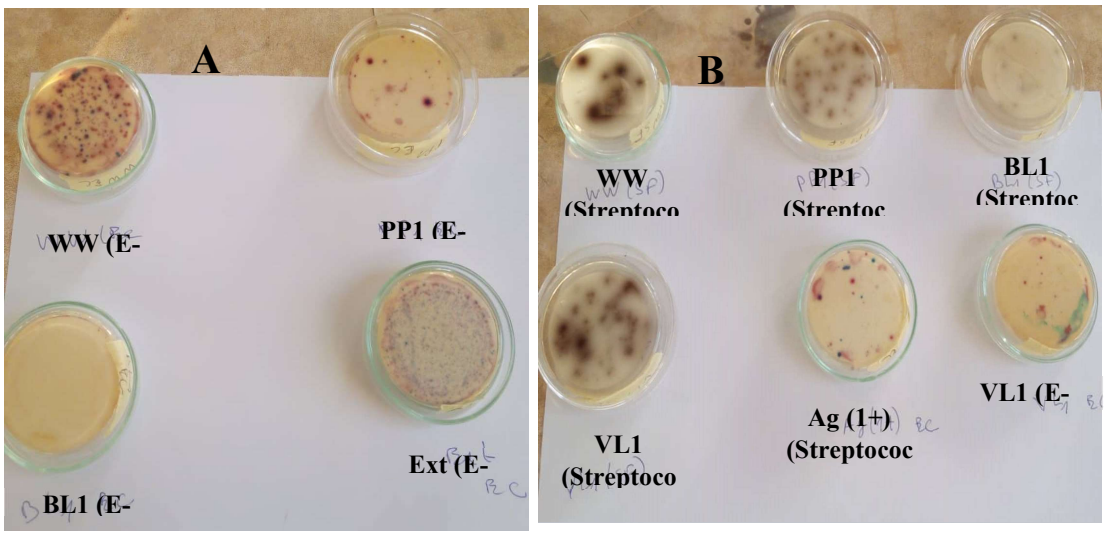

Figure 8. Diffusion analysis of the wastewater and treated water samples against (A) *E. coli*, (B) *Streptococci*

From raw wastewater analysis, it was observed that the mean count for *Fecal Streptococci* (FS) was 12 x 103 CFU/100 ml and *Escherichia coli* (EC) was 47 x 103 CFU/100 ml. These counts decreased with the addition of nanoparticles produced from the three plant extracts and silver nitrate, but remained unchanged with the addition of the plant extracts.

Figure 9 presents the *E. coli and Streptococcus bacterial counts in all water samples, corresponding to the nanoparticles' ability* to eliminate each bacterium. It can be observed from the analysis that the mean value of the *E. coli* was relatively high in the raw wastewater, and was reduced upon addition of the different nanoparticles and AgNO3 solution. The *E. coli* elimination efficiency for the various nanoparticles were 99.6% for the nanoparticles produced with paw-paw plant (PNP), 98.1% with Perilla mint nanoparticles (VNP), and 100% removal efficiency with the bitter leaf nanoparticles (BNP). The AgNO3 solution was observed to have an E. coli elimination efficiency of 89.8%. The highest elimination efficiency of *E. coli* was

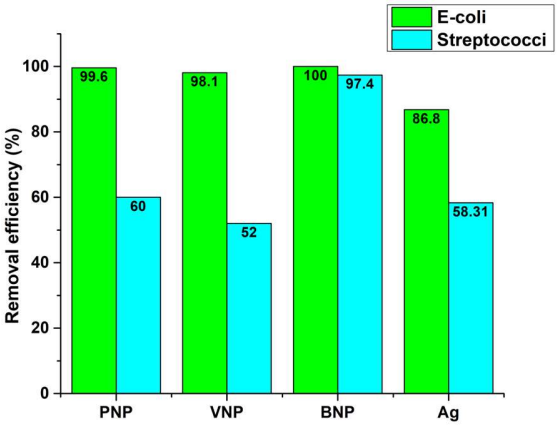

Figure 9. Antibacterial activities of Ag-NP against *E. coli* and *Streptococci*

obtained from the silver nanoparticles produced with bitter leaf (BNP).

Similarly, with the addition of Silver nanoparticles produced from various plant extracts, the counts of Streptococci reduced with an elimination efficiency of 60% in PNP, 52.5% in VNP, and 97.42% in BNP. Furthermore, the *Streptococci* elimination efficiency for $AgNO_3$ solution was found to be 58.31%. The addition of each plant extract had no notable effect on the microbes in wastewater.

The observed results indicate that the synthesized Ag-NPs are suitable for inhibiting the activities of microorganisms like *E. coli*, *Streptococci,* and possibly other microbes in wastewater. The aforementioned results also reveal that Ag-NPs synthesized from the different plants had different degrees of antibacterial activities on different microbes, and the Ag-NPs produced from bitter leaf (BNP) had the highest antibacterial activity of the three. This confirms that, as the phytochemistry of the plant affects its kinetics of production, so does it affect its antibacterial properties. The use of Ag-NP will therefore find extensive use in water and wastewater treatment.

4. CONCLUSION

In the synthesis of metal nanoparticles through bio-reduction, silver nanoparticles (Ag-NPs) have gained a lot of interest due to their formidable properties and good antimicrobial characteristics. This study seeks to determine the characteristics and antibacterial properties of Ag-NPs produced from different plants. Three plants were selected, ie, *Carica papaya* (Paw-paw plant), *Vernonia* amygdalina (Bitter leaf plant), and *Perilla frustescens var* (Perilla mint plant) as reducing and capping agent, and 6 mM silver nitrate as precursor. The synthesized NPs were characterized through optical microscopy, UV-Vis spectroscopy, FTIR, XRD, particle size distribution, and zeta potential. The confirmation of the formation of Ag-NPs was revealed by the UV-Vis spectroscopy, with the Surface Plasmon Resonance between 410 and 440 nm, and the most intense being VNP and BNP. XRD revealed the strong crystalline nature of the Ag-NPs synthesized from all three plant extracts. The optical microscopy observation of Ag-NPs showed the presence of NPs formed, slightly dispersed with zone aggregation. By means of zeta potential, it was seen that the average surface charge of all the nanoparticles was negative, and less than -10 mV, indicating weak inter-repulsion between nanoparticles, hence strong affinity for aggregation. This was confirmed through their particle size distribution. In the treatment of urban wastewater, all three Ag-NPs had the affinity to eliminate *E. coli* and *Streptococci* in wastewater. BNP had the best inhibiting capacity, followed by PNP and finally VNP. Hence, NP produced in the same conditions from different plant extracts exhibit different degrees of antibacterial properties. In summary, the application of biosynthesized nanoparticles can pass its laboratory phase into a standard water and wastewater treatment system.

Acknowledgement

The authors thank the Local Materials Promotion Authority (MIPROMALO) for providing laboratory facilities to carry out this research.

Funding

The authors of the manuscript did not receive any funding or grants for this work.

Credit authorship contribution statement

Elton Yerima: Investigator, Writing-Original draft. **Julson Ahmed Tchio**: Analysis. **Tsamo Cornelius**: Supervisor and conceptualization. **Elie Kamseu**: Supervisor.

Conflict of Interest

The authors declare that they have no known competing financial interests or personal relationships that could have appeared to influence the work reported in this paper.

5. REFERENCES

[1] B. K. Narayanan, S. Natarajan, Biological synthesis of metal nanoparticles by microbes, *Adv. Colloid Interface Sci.*, 156 (2010), pp. 1–13

[2] P. Mukherjee, M. Roy, B. P. Mandal, G. K. Dey, P. K. Mukherjee, J. Ghatak, A. K. Tyagi, S. P. Kale, Green synthesis of highly stabilized nanocrystalline silver particles by a non-pathogenic and agriculturally important fungus *T. Asperellum*, *Nanotechnol.*, 19 (2008) 7, doi 10.1088/0957-4484/19/7/075103p 7.

[3] T. M. Mohammed, Removal of pathogenic bacteria from wastewater using silver nanoparticles synthesized by two fungal

species, *Water Science*, 31 (2017) 2, https://doi.org/10.1016/j.wsj.2017.11.001

[4] V. Arya, Living systems eco-friendly nanofactories, *Dig. J. Nanomater. Biostruct.*, 5 (2010) 1. pp 9–21

[5] D. M. Ali, M. Sasikala, M. Gunasekaran, N. Thajuddin, Biosynthesis and characterization of silver nanoparticles using marine Cyanobacterium oscillatoria, *Dig. Journal of Nanomater. Biostruct*, 6 (2011) 2, pp 385–390

[6] R. E. Sardjono, R. Gunawan, B. Anwar, Erdiwansyah, R. Mamat, A Mini Review: Biosynthesis of Silver Nanoparticles and Its Activity as Antioxidant, *Moroccan Journal of Chemistry,* 10 (2022) 4. pp 808–821. https://doi.org/10.48317/IMIST.PRSM/morjchem-v10i3.30801

[7] S. Anjum, J. Gideon, G. Bhuvanesh, Investigation of the herbal synthesis of silver nanoparticles using Cinnamon zeylanicum extract, *Emergent Materials*, 2 (2019), pp 113–122, https://doi.org/10.1007/s42247-019-00023-x

[8] J. Bhaumik, N. S. Thakur, P. K. Aili, A. Ghanghoriya, A. K. Mittal, U. C. Banerjee, *ACS Biomater. Sci. Eng.*, 1 (2015) 6, p. 382

[9] N. S. Thakur, J. Bhaumik, S. Kirar, U. C. Banerjee, *ACS Sustain. Chem. Eng.*, 5 (2017) 9, p. 7950

[10] S. Y. Lee, S. Krishnamurthy, C. W. Cho, Y. S. Yun, Biosynthesis of gold nanoparticles using *Ocimum sanctum* extracts by solvents with different polarity, *ACS Sustain. Chem. Eng.*, 4 (2016) 5, pp. 2651–2659, https://doi.org/10.1021/acssuschemeng.6b00161

[11] M. Bahwirth, S. Bamsaoud, The effect of silver nanoparticles on the germination and growth of two cultivars of wheat, *Triticum aestivum* L. Alandalus, *Journal of Applied Science*, 7 (2020) 11, pp. 7–25

[12] S. F. Bamsaoud, M. A. Bahwirth, The effect of biologically synthesized silver nanoparticles on the germination and growth of *Cucurbita pepo* seedlings, *Journal of the Arab American University*, 3 (2017) 2, pp. 34– 47

[13] T. Tenzin, A. Kaur, Recent Advances in the Green Synthesis of Gold and Silver Nanostructures for Augmented Anti-Microbial Activity, *Iranian Journal of Materials Science and Engineering*, 19 (2022) 2, pp. 1- 28 https://doi.org/10.22068/ijmse.2252

[14] S. Dimitrieska, A. Stankovska, T. Efremova, The Fourth Industrial Revolution Advantages and Disadvantages, *Economics and Management*, 14 (2018) 2, pp. 182–187

[15] M. M. Basuliman, A. S. Bamahel, D. G. Al-Kathiri, A. M. Al-Suhily, The Effect of Various Concentrations of $AgNO_3$ Aqueous Solutions on Silver Nanoparticles Biosynthesis Using *Tarchonanthus Camphoratus* Leaf Extract and Their Antibacterial Activity, *Mor. Journal of. Chememistry*, 14 (2023) 2, pp. 361-370. Doi: https://doi.org/10.48317/IMIST.PRSM/morjchem-v11i1.33269

[16] P. Logeswari, S. Silambarasan, J. Abraham, Synthesis of silver nanoparticles using plant extract and analysis of their antimicrobial property, *Journal of Saudi Chemical Society,* 19(2012) 3, pp. 311-317 http://dx.doi.org/10.1016/j.jscs.2012.04.007

[17] E. S. H. Haridas, M. K. R. Varma, G. K. Chandra, Bioactive silver nanoparticles derived from *Carica papaya* floral extract and its dual-functioning biomedical application, *Science Report,* (2025) 15, p. 9001 https://doi.org/10.1038/s41598-025-93864-y

[18] G. Z. Jahangir, T. Anjum, N. Rashid, M. Sadiq, R. Farooq, M. Akhtar, S. Hussain, A. Iftikhar, M. Z. Saleem, R. S. Shaikh, *Carica papaya* Crude Extracts are an Efficient Source of Environmentally Friendly Biogenic Synthesizers of Silver Nanoparticles, *Sustainability,* 15(2023) 24, p. 16633, https://doi.org/10.3390/su152416633.

[19] R. C. Omeh, I. J. Ali, C. C. Adonu, *Venonia amygdalina* leaf extract - mediated redox synthesis of silver nanoparticles: Characterization and antimicrobial activity, *German Journal of Pharmaceuticals and Biomaterials*, 2 (2023) 4, pp. 19-30

[20] J. Balavijayalakshmi, V. Ramalakshmi, *Carica papaya* peel mediated synthesis of silver nanoparticles and its antibacterial activity against human pathogens, *Journal of Applied Research and Technology,* 15 (2017) 5, pp. 413-422 https://doi.org/10.1016/j.jart.2017.03.010.

[21] A. C. Ovenseri, O. A. Johnbull, Formulation of silver nanoparticles from the leaves extract of *Vernonia amygdalina*, *The Nigerian Journal of Pharmacy*, 57 (2023) 1, pp. 459 – 466, https://doi.org/10.51 412/psnnjp.2023.7

[22] M. Tavan, P. Hanachi, M. H. Mirjalili et al., Comparative assessment of the biological activity of the green synthesized silver nanoparticles and aqueous leaf extract of *Perilla frutescens* (L.), *Science Report,* 13 (2023), 6391 https://doi.org/10.1038/s41598-023-33625-x

[23] S. O. Aisida, K. Ugwu, P. A. Akpa, A. C. Nwanya, U. Nwankwo, S. S. Botha, P. M. Ejikeme, I. Ahmad, M. Maaza, F. I. Ezema, Biosynthesis of silver

nanoparticles using bitter leaf (*Veronica amygdalina*) for antibacterial activities, *Surfaces and Interfaces*, 17 (2019), 100359– https://doi.org/10.1016/j.surfin.2019.100359.

[24] A. A. O. Sirajudeen, J. F. Sanusi, O. A. Akintola, A. O. Sakariyau, O. F. Adesina, S. Bankole, Eco-Friendly Production of Silver Nanoparticles from *Vernonia amygdalina* and *Citropsis articulata*: An Assessment of Antibacterial Properties against Oral Bacteria, *Journal of Medical Microbiology and Infectious Diseases*, 12 (2024) 1, pp. 22 -34 https://doi.org/10.61186/JoMMID.12.1.22. ,

[25] T. Hou, Y. Guo, W. Han, Y. Zhou, V. R. Netala, H. Li, H. Li, Z. Zhang, Exploring the Biomedical Applications of Biosynthesized Silver Nanoparticles Using *Perilla frutescens* Flavonoid Extract: Antibacterial, Antioxidant, and Cell Toxicity Properties against Colon Cancer Cells, *Molecules, 28* (2023), 17, pp. 6431 https://doi.org/10.3390/molecules28176431

[26] M. Firdaus, S. Andriana, Elvinawati, W. Alwi, E. Swistoro, A. Ruyani, A. Sundaryono, Green synthesis of silver nanoparticles using *Carica Papaya* fruit extract under sunlight irradiation and their colorimetric detection of mercury ions. *Journal of Physics: Conference Series*, 817 (2017) 1, 012029 https://doi.org/10.1088/1742-6596/817/1/012029

[27] S. F. Bamsaoud, M. M. Basuliman, E. A. Bin-Hameed, S. M. Balakhm, A. S. Alkalali, The effect of volume and concentration of $AgNO_3$ aqueous solutions on silver nanoparticles synthesized using *Ziziphus Spina* – Christi leaf extract and their antibacterial activity, *Journal of Physics: Conference Series*, Volume 1900, The 1st International Conference on Fundamental, Applied Sciences and Technology (ICoFAST 2021), 15-16 March 2021, (Perlis, Malaysia), (Hadhramout, Yemen) https://doi.org/10.1088/1742-6596/1900/1/012005.

[28] R. Sarkar, P. Kumbhakar, A. K. Mitra, Green Synthesis of Silver Nanoparticles and Its Optical Properties, *Digest Journal of Nanomaterials and Biostructures*, 5 (2010) 2, pp. 491 – 496

[29] M. Ansari, S. Ahmed, A. Abbasi, M. T. Khan, M. Subhan, N. A. Bukhari, A. A. Hatamleh, N. R. Abdelsalam, Plant-mediated fabrication of silver nanoparticles, process optimization, and impact on tomato plant, Scientific Reports, 13(2023):18048 https://doi.org/10.1038/s41598-023-45038-x.

[30] G. A. Martínez-Castañón, N. Niño-Martínez, F. Martínez-Gutiérrez, J. R. Martínez-Mendoza, F. Ruiz, *Journal of Nanoparticle Resources*, 10 (2008), 1343

[31] S. Pugazhendhi, P. Sathya, P. K. Palanisamy, R. Gopalakrishnan, Synthesis of silver nanoparticles through green approach using *Dioscorea alata* and their characterization on antibacterial activities and optical limiting behavior, *Journal of Photochemistry and Photobiology B: Biology*, 159 (2016), pp. 155-160

[32] E. A. A. Kareem, H. M. Oraibi, A. E. Sultan, Synthesis and Characterization of Silver Nanoparticles: A Review. *Ibn Al-Haitham Journal for Pure and Applied Sciences*, IHJPAS.. 36 (2023) 3, https://doi.org/10.30526/36.3.3050.

[33] N. Jain, A. Bhargava, S. Majumdar, J. C. Tarafdarb, J. Panwar, *Nanoscale*, 3 (2011), 635

[34] D. T. Stalin, In vitro antibacterial activity of biosynthesized silver nanoparticles against Gram-negative bacteria, *Inorganic and Nano-Metal Chemistry*, 2022, pp. 1-10.

[35] Z. Hashemi, Z. M. Mizwari, S. Mohammadi-Aghdam, S. Mortazavi-Derazkola, M. A. Ebrahimzadeh, Sustainable green synthesis of silver nanoparticles using *Sambucus ebulus phenolic* extract (AgNPs@ SEE): Optimization and assessment of photocatalytic degradation of methyl orange and their in vitro antibacterial and anticancer activity, *Arabian Journal of Chemistry,* 15 (2022) 1, 103525

[36] S. Palithya et al., Green synthesis of silver nanoparticles using flower extracts of *Aerva lanata* and their biomedical applications, *Particle Science and Technol.,* 40 (2022) 1, pp. 84–96

[37] A. Dhaka, S. C. Mali, S. Sharma, R. A.Trivedi, Review on biological synthesis of silver nanoparticles and their potential applications, *Results in Chemistry,* 6 (2023) 101108 https://doi.org/10.1016/j.rechem.2023.101108

[38] K. Kayed, M. Issa, H. Al-ourabi, The FTIR spectra of Ag/Ag_2O Composites Doped with Silver Nanoparticles, *Journal of Experimental Nanoscience,* 19 (2024) 1, 2336227 https://doi.org/10.1080/17458080.2024.2336337

[39] M. Asif, R. Yasmin, R. Asif, A. Ambreen, M. Mustafa, S. Umbreen, Green Synthesis of Silver Nanoparticles (AgNPs), Structural Characterization, and their Antibacterial Potential, *Dose-Response: An International Journal*, 20 (2022) 2 https://doi.org/10.1177/15593258221088709

[40] L. W. Zhang, N. A. Monteiro-Riviere, Use of confocal microscopy for nanoparticle drug

delivery through skin, *Journal of Biomedical Optics,* 18(2013) 6:061214. https://doi.org/10.1117/1.JBO.18.6.061214

[41] A. Al-Zubeidi, L. A. McCarthy, A. Rafiei-Miandashti, T. S. Heiderscheit, S. Link, Single-particle scattering spectroscopy: fundamentals and applications, *Nanophotonics*, 10 (2021) 6, pp. 1621–1655 https://doi.org/10.1515/nanoph-2020-0639

[42] Malvern. Technical notes: Zeta potential – Introduction in 30 minutes. Malvern Instrument Limited. 2015, https://www.research.colostate.edu/wp-content/uploads/2018/11/zetapotential-introduction-in-30min-Malvern.pdf. (Accessed November 02, 2025)

[43] A. Almatroudi, Silver nanoparticles: synthesis, characterization, and biomedical applications. *Open Life Science*, 15 (2020) 1. pp. 819-839. https://doi.org/10.1515/biol-2020-0094. PMID: 33817269; PMCID: PMC7747521.

[44] C. Gibson, Investigating Initial Interactions between Silver Nanoparticles and Wastewater. Biological and Agricultural Engineering Undergraduate Honors Theses (2018). Retrieved from https://scholarworks.uark.edu/baeguht/47. (Accessed 02 November 2025)